

# Toward Large Arrays of Multiplex Functionalized Carbon Nanotube Sensors for Highly Sensitive and Selective Molecular Detection

Pengfei Qi, Ophir Vermesh, Mihai Grecu, Ali Javey, Qian Wang, and Hongjie Dai\*

*Department of Chemistry, Stanford University, Stanford, California 94305*

Shu Peng and K. J. Cho

*Department of Mechanical Engineering, Stanford University, Stanford, California 94305*

*Received January 7, 2003; Revised Manuscript Received January 16, 2003*

## ABSTRACT

Arrays of electrical devices with each comprising multiple single-walled carbon nanotubes (SWNT) bridging metal electrodes are obtained by chemical vapor deposition (CVD) of nanotubes across prefabricated electrode arrays. The ensemble of nanotubes in such a device collectively exhibits large electrical conductance changes under electrostatic gating, owing to the high percentage of semiconducting nanotubes. This leads to the fabrication of large arrays of low-noise electrical nanotube sensors with 100% yield for detecting gas molecules. Polymer functionalization is used to impart high sensitivity and selectivity to the sensors. Polyethyleneimine coating affords n-type nanotube devices capable of detecting NO<sub>2</sub> at less than 1 ppb (parts-per-billion) concentrations while being insensitive to NH<sub>3</sub>. Coating Nafion (a polymeric perfluorinated sulfonic acid ionomer) on nanotubes blocks NO<sub>2</sub> and allows for selective sensing of NH<sub>3</sub>. Multiplex functionalization of a nanotube sensor array is carried out by microspotting. Detection of molecules in a gas mixture is demonstrated with the multiplexed nanotube sensors.

The electrical conductance of semiconducting SWNTs (band gaps  $\sim 0.5$  eV) can vary by orders of magnitude under electrostatic gating or doping. This serves as the basis for nanotube field effect transistors (FETs).<sup>1–4</sup> SWNTs are molecular wires with every atom on the surface. Charge transfer between SWNTs and adsorbed molecules could cause drastic changes to the nanotube conductance, a chemical gating effect that can be utilized for molecular sensing,<sup>5</sup> as initially demonstrated by Kong et al. for NO<sub>2</sub> and NH<sub>3</sub> detection.<sup>6</sup> Nanotube sensors offer significant advantages over conventional metal-oxide-based electrical sensor materials in terms of sensitivity, room temperature operation, and small sizes needed for miniaturization and construction of massive sensor arrays. Nevertheless, several outstanding issues remain. First, for sensing purposes, it is desired to reliably obtain devices consisting of only semiconductor SWNTs (one or multiple), as the electrical properties of metallic SWNTs are relatively insensitive to chemical gating.<sup>6,7</sup> This requires growing only semiconducting SWNTs through chirality control, an ability currently lacking for synthesis methods. Second, strategies should be

devised to impart selectivity to nanotube sensors, a task that will ultimately determine the practical usefulness of these devices.

Here, we present our recent results in tackling the issues above. We show that large arrays of devices containing multiple SWNTs bridging electrodes can be easily produced with 100% yield by CVD growth of nanotubes from micropatterned catalyst. The ensemble of SWNTs in each device collectively exhibits substantial electrical conductance changes to electrostatic gating, owing to the high percentage of semiconducting nanotubes grown by CVD. The multiplexed devices (referred to as MT devices from here on) are highly sensitive to chemical gating effects and, importantly, exhibit lower electrical noise than individual semiconducting SWNT devices. Large arrays of nanotube chemical sensors with excellent characteristics are thus obtainable. Further, we have carried out polymer functionalization of the MT devices to afford ultrahigh sensitivity for NO<sub>2</sub> detection and impart selectivity to nanotube sensors. We demonstrate that microspotting allows for functionalization of nanotube sensor arrays in a multiplex fashion, enabling detection of molecules in gas mixtures.

\* Corresponding author. E-mail: hdai@stanford.edu.

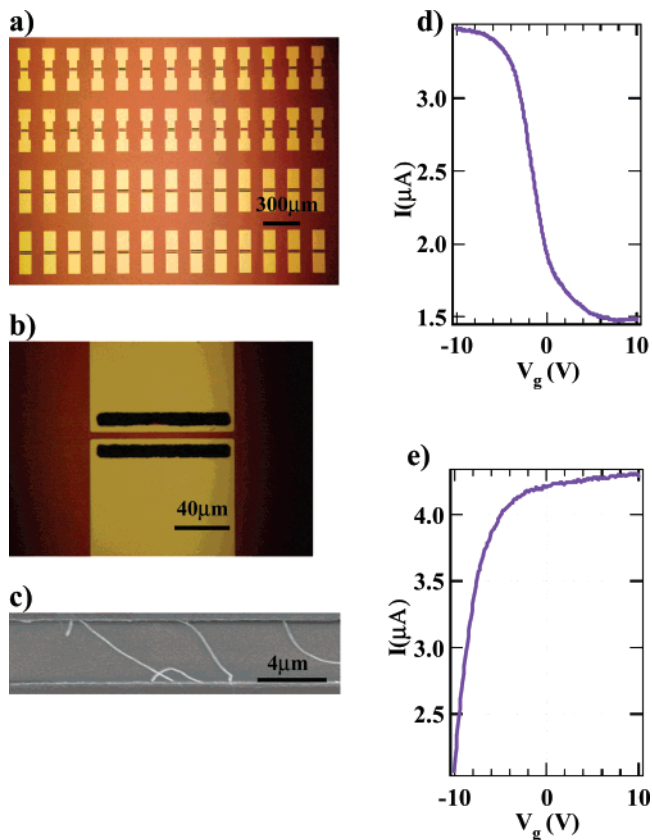


**Figure 1.** (a) Optical image of an array of multiple-SWNT devices. (b) Optical image of one device. The black regions ( $100\ \mu\text{m}$  long) contain catalyst patterned on top of opposing Mo source and drain electrodes. (c) Scanning electron microscopy (SEM) image of several nanotubes bridging two opposing Mo electrodes in a device. The operating voltage used for our field emission SEM is low (1 kV) to reduce surface charging. The nanotubes appear bright and the apparent widths do not correspond to the true diameter of the nanotubes (average  $\sim 2\ \text{nm}$  measured by AFM and TEM). (d)  $I-V_g$  characteristics of an as-grown MT device. Source-drain bias voltage = 10 mV. (e)  $I-V_g$  curve recorded for the device after PEI functionalization of the device.

Our device fabrication followed that described previously by CVD growth<sup>8</sup> of SWNTs across an array of preformed metal (Mo) electrodes from patterned catalyst on a Si/SiO<sub>2</sub> substrate (Figure 1).<sup>9</sup> The thickness of the thermal SiO<sub>2</sub> was 500 nm, and the underlying doped Si substrate was used as back-gate for the nanotubes. Importantly, the width of patterned catalyst regions was large,  $\sim 100\ \mu\text{m}$  in the current work, allowing for the growth of a large number of SWNTs across the electrodes (Figure 1b,c). Characterization by microscopy revealed that the average number of tubes in each device was  $\sim 20\text{--}30$ . After CVD growth, electrical probing of the arrays revealed that devices with multiple-SWNT connections were reproducibly obtained with 100% yield. From current vs gate voltage ( $I-V_g$ ) measurements, we found that the ensemble of SWNTs in each device appeared p-type, exhibiting an overall electrical conductance decrease by a factor of 2–3 when  $V_g$  was swept from  $-10$  to  $10\ \text{V}$  (Figure 1d). The sensitivity of the MT devices to electrostatic gating suggested a high percentage of semiconductor SWNTs in the MT devices, consistent with previous finding for CVD grown tubes.<sup>10</sup> The nonelectrical depletion of MT devices

at positive gate voltage was due to conduction of small percentages of metallic nanotubes in the ensemble. This differed from individual semiconducting SWNT devices that exhibited orders of magnitude conductance decrease under the same  $V_g$  sweep.

A significant advantage of the multiple-tube devices over individual tubes was lower electrical noise, desired for electrical sensing. The  $I-V_g$  curves for the MT devices were smooth, without the superimposed telegraph noise often observed with individual tube devices. When monitoring conductance as a function of time (under  $V_g = 0$ ), we typically observed  $\sim 1\%$  fluctuations for the MT devices and  $\sim 10\%$  or more fluctuations<sup>6</sup> for individual nanotubes. The lower noise level for MT devices was attributed to the larger number of tubes ( $N$ ) in the devices since noise scales as  $1/N$ .<sup>11</sup> The as-grown MT devices were tested for gas sensing and exhibited excellent sensitivity to NO<sub>2</sub>. The electrical conductance of a typical MT device increased by  $\sim 80\%$  when exposed to 100 ppb of NO<sub>2</sub> in Ar due to hole doping by adsorbed molecules. This result was highly reproducible with different batches of MT devices. Since the MT devices are simple to prepare, high yield, electrically stable with low noise, and highly sensitive to molecular gating, we conclude that it is not necessary to restrict to individual semiconducting nanotubes in pursuing sensor applications.

We investigated functionalization of nanotubes in the MT devices by various polymers for enhancing sensitivity and imparting selectivity to nanotube sensors. For an example, we adsorbed polyethyleneimine (PEI, Aldrich Chemicals) onto SWNTs in MT devices by simple immersion in a 20 wt % PEI/methanol solution for 2 h, rinsed with methanol, and then baked at  $50\ ^\circ\text{C}$  for 1 h. The PEI-coated MT devices evolved into n-type (Figure 1e) due to electron transfer doping by high-density amine groups on PEI, similar to that observed with individual semiconducting SWNTs.<sup>12</sup> The PEI functionalized n-type MT devices were ultrasensitive to NO<sub>2</sub> (Figure 2a), responding to as low as 100 ppt (parts per trillion) of NO<sub>2</sub> (vs  $\sim 10\text{--}50\ \text{ppb}$  for as-grown MT devices) with an appreciable conductance decrease. The lowest concentrations of NO<sub>2</sub> reliably detected by the n-type MT devices are several ppb with a response time of  $\sim 1\text{--}2\ \text{min}$  (defined as the time for 80% conductance change to take place). The conductance change vs NO<sub>2</sub> concentration showed a linear dependence for  $[\text{NO}_2] = 100\ \text{ppt}$  to 3 ppb and a tendency of saturation for higher  $[\text{NO}_2]$  (Figure 2b). The data in Figure 2a were recorded successively for various  $[\text{NO}_2]$ , and the sensor recovery was done by desorbing NO<sub>2</sub> with ultraviolet (UV) light illumination.<sup>13</sup> The conductance of the n-type MT devices decreased upon NO<sub>2</sub> binding (as opposed to increasing for as-grown p-type device) due to electron transfer to NO<sub>2</sub> reducing the majority carriers in the nanotubes. The  $I-V_g$  curves recorded for the MT device exposed to various NO<sub>2</sub> concentrations shifted progressively to the positive  $V_g$  side, accompanied by reduced n-channel conductance (Figure 2c), consistent with the charge-transfer scenario. Similar threshold voltage shifts by NO<sub>2</sub> adsorption on individual PEI functionalized n-type semiconducting SWNTs were also observed.

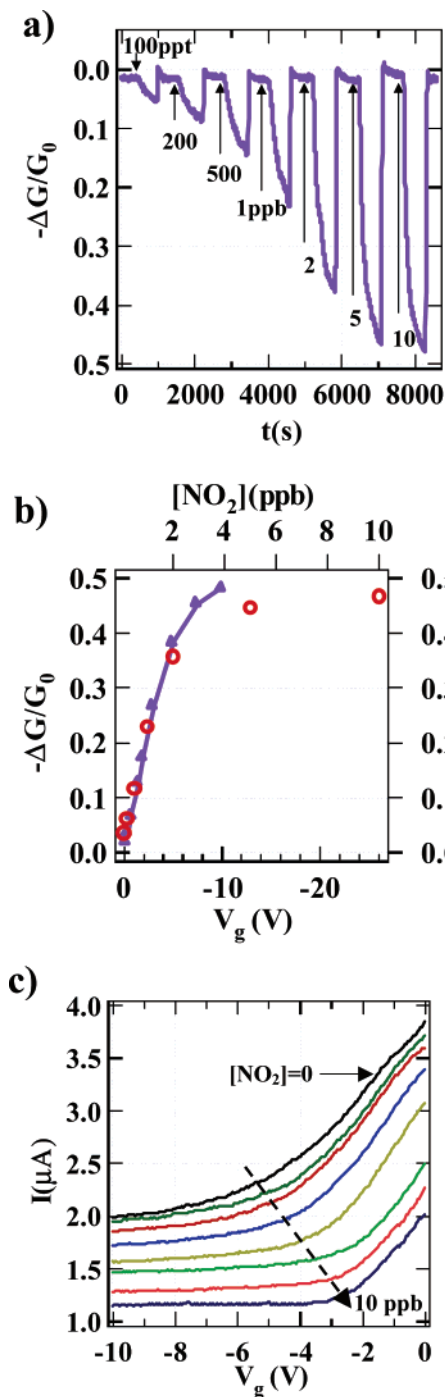


**Figure 2.** (a) Change in conductance normalized by initial conductance ( $G_0$ ) at  $V_g = 0$  as a function of time for a PEI-functionalized n-type MT device exposed to various concentrations of  $\text{NO}_2$  gas. The device was exposed to each concentration of  $\text{NO}_2$  for 10 min, after which recovery was made by UV light (254 nm) desorption of  $\text{NO}_2$ .<sup>13</sup> The concentration of  $\text{NO}_2$  was varied by diluting 100 ppm of  $\text{NO}_2$  (in Ar) with air by using four mass-flow controllers. The diluted gas was then flown into a homemade chamber that houses the sensor chip. (b) Conductance change vs concentration of  $\text{NO}_2$  (top horizontal axis, data points in circles) and conductance vs gate-voltage (bottom axis, data points in triangles) respectively for an n-type MT device. (c)  $I-V_g$  curves for a device recorded after exposure to  $\text{NO}_2$  of successively increasing concentrations (from black curve to blue curve:  $[\text{NO}_2] = 0, 0.1, 0.2, 0.5, 1, 2, 5, 10$  ppb respectively).

$\text{NO}_2$  detection at concentrations  $\leq 1$  ppb with PEI-coated SWNTs represents the first time electrical sensors detected

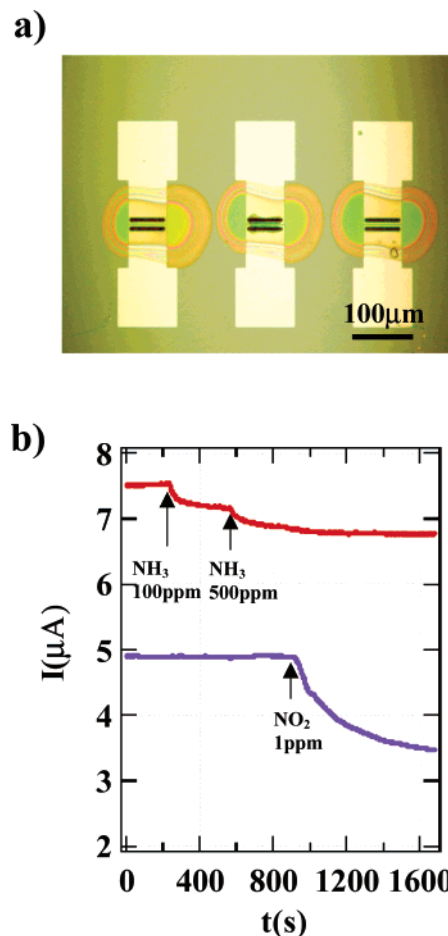


**Figure 3.** (a) Optical image showing three MT devices after microspotting with droplets of polymer solutions. (b) Red (top) curve: a device coated with Nafion exhibits response to 100 and 500 ppm of  $\text{NH}_3$  in air, and no response when 1 ppm of  $\text{NO}_2$  was introduced to the environment. Blue (bottom) curve: a PEI-coated device exhibiting no response to 100 and 500 ppm of  $\text{NH}_3$  and large conductance decrease to 1 ppm of  $\text{NO}_2$ .

molecules at such low levels that typically require spectroscopy techniques.<sup>14</sup> As shown in a later analysis, the PEI functionalization renders as-grown SWNTs electron rich, leading to higher binding affinity and sticking coefficient for the electron-withdrawing  $\text{NO}_2$ . Importantly, the PEI-coated MT devices exhibit no response when exposed to  $\text{NH}_3$ , a weakly electron-donating molecule for up to 1% concentrations (as-grown tubes readily respond to  $\sim 100$  ppm of  $\text{NH}_3$ ). This  $\text{NH}_3$  insensitivity is attributed to low binding affinity and sticking coefficient of  $\text{NH}_3$  on the electron-rich (due to high-density amines on PEI) n-type SWNTs. The PEI-functionalized MT devices also exhibit no change of electrical conductance when exposed to many other molecules including  $\text{CO}$ ,  $\text{CO}_2$ ,  $\text{CH}_4$ ,  $\text{H}_2$ , and  $\text{O}_2$ . These results show that PEI functionalized SWNTs are highly selective to strongly electron withdrawing molecules. Future work will be aimed at imparting selectivity to nanotube sensors for  $\text{NO}_2$ ,  $\text{SO}_2$ , and  $\text{O}_3$  that have similar electron withdrawing properties.

We also explored selective detection of  $\text{NH}_3$  with the MT devices and found that coating an as-grown MT device with Nafion blocks certain types of molecules from reaching

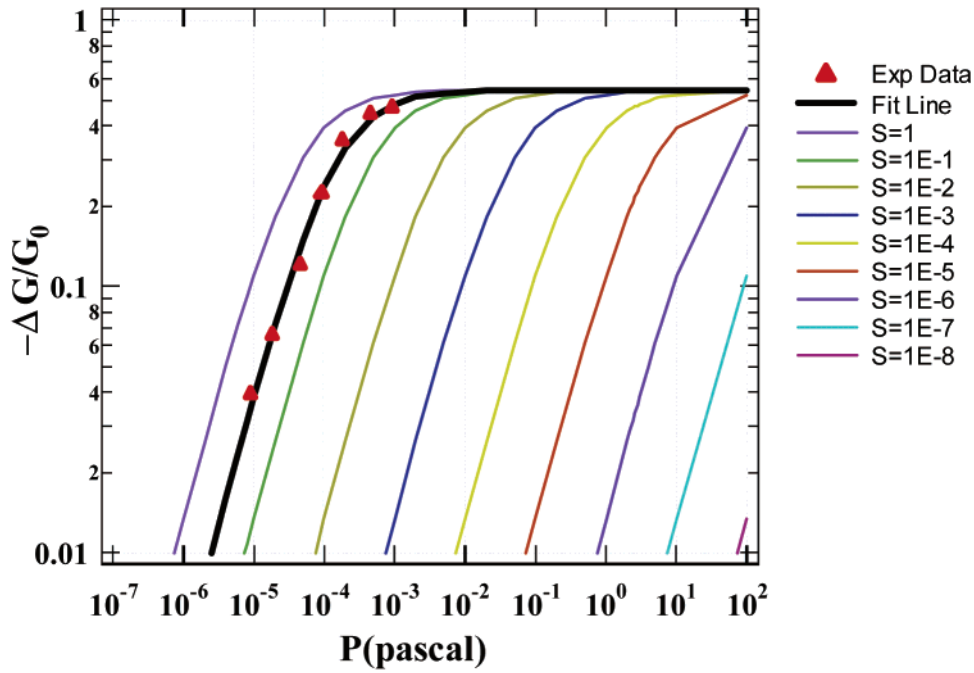


**Figure 4.** Calculated  $\Delta G/G_0$  for n-type SWNT sensors versus  $\text{NO}_2$  partial pressure (P) for  $\text{NO}_2$  sticking coefficient (S) ranging from 1 to  $10^{-8}$ . The solid triangles are experimental data. Comparison between calculation (see the fit line) and experimental result suggest that the sticking coefficient  $S \sim 0.3$ .

nanotubes, including  $\text{NO}_2$ . This allows for  $\text{NH}_3$  detection in a more selective manner. Nafion is a polymer with a Teflon backbone and sulfonic acid side groups, and is well-known to be perm-selective to  $-\text{OH}$ -containing molecules including  $\text{NH}_3$ <sup>15</sup> that tend to react with  $\text{H}_2\text{O}$  in the environment to form  $\text{NH}_4\text{OH}$ . Further, we used microspotting to coat MT devices in an array with different polymers, aimed at detecting  $\text{NO}_2$  and  $\text{NH}_3$  in gas mixtures with multiplex-functionalized nanotube sensors. Microspotting of polymer solutions was done with a commercial micropin (Telechem International Inc.) mounted on an in-house micromanipulator equipped with an optical microscope that allowed for positioning the pin over the MT devices (Figure 3a). Figure 3b shows that the conductance of a Nafion-coated device (spotted with 1% Nafion in a water droplet) decreases (due to  $\text{NH}_3$  electron donation to the p-type device reducing the majority hole carriers), while a PEI-coated (0.1% in the water droplet) device on the same chip shows no response to  $\text{NH}_3$ . When introducing 1 ppm of  $\text{NO}_2$  into the environment with the presence of 500 ppm of  $\text{NH}_3$ , the Nafion-coated device exhibits no response while the PEI-coated device shows a significant conductance decrease. These results clearly demonstrate that multiplexed nanotube sensor arrays are promising for detecting multiple molecules in complex chemical environments.

The molecular sensing mechanisms for as-grown SWNTs have been investigated by a number of experimental and theoretical groups.<sup>6,16–20</sup> Charge-transfer doping of opposite directions was reported for  $\text{NO}_2$  and  $\text{NH}_3$  by Kong et al. based on threshold voltage shifts of individual semiconducting nanotubes.<sup>6</sup> Several theoretical works have revealed the binding energies and charge transfer for  $\text{NO}_2$  (binding energy  $E_b$  ranges from 0.3 to 0.8 eV; charge transfer  $\sim 0.06$  to 0.3

$|e|$  from tube to molecule) and  $\text{NH}_3$  ( $E_b \sim 0.15$  to 0.18 eV; charge transfer 0.03 to 0.04  $|e|$  from molecule to tube) for the (10,0) tube.<sup>17,19</sup> A consensus is still lacking about the precise values due to different computation methods. For  $\text{NH}_3$ , our initial density-functional theory (DFT) calculation (without nanotube and  $\text{NH}_3$  relaxation) observed nonbinding states for  $\text{NH}_3$  and SWNT,<sup>6</sup> and more recently, refined calculations (with nanotube and  $\text{NH}_3$  fully relaxed) revealed a binding energy of  $\sim 0.1$  to 0.2 eV (depending on binding configuration) and electron donation of 0.06  $|e|$  by  $\text{NH}_3$  to a (8,0) SWNT (S. Peng, K. J. Cho, unpublished result), in agreement with the calculated results by other groups.<sup>17,19</sup> An importantly recent development is that  $\text{NO}_2$  and  $\text{NH}_3$  binding to SWNTs and opposite directions of charge-transfers for these molecules have been confirmed by X-ray photoemission spectroscopy measurements.<sup>20</sup>

We have analyzed our  $\text{NO}_2$  sensing data obtained with the PEI-coated n-type SWNT devices. Assuming a Langmuir isotherm<sup>21</sup> and since  $[p/(2\pi mk_B T)^{1/2}]AS(1 - \theta) \approx (A/\sigma)\theta v \exp(-E_b/k_B T)$  at the  $\text{NO}_2$  adsorption and desorption equilibrium (for a given partial pressure  $p$ ), we obtain that the coverage of  $\text{NO}_2$  on the nanotube is given by

$$\theta(p) = 1/\{1 + [(2\pi mk_B T)^{1/2} v \exp(-E_b/k_B T)]/pS\sigma\}$$

where  $m$  is the molecular mass,  $T = 300$  K,  $A$  is the nanotube surface area,  $S$  is the sticking coefficient,  $\sigma \sim 10^{-19}$   $\text{m}^2$  is the molecular cross-section, and  $v \sim 10^{12}$ /s and  $E_b$  are the molecular vibration frequency and binding energy respectively (the desorption rate  $\sim \exp[-E_b/k_B T]$  is approximated by the transition state theory<sup>21</sup>). Assuming  $\Delta G \propto \theta$  for low  $[\text{NO}_2]$  in the linear region (Figure 2b) and  $E_b \sim 0.8$  eV, our calculations of  $\Delta G$  vs  $p$  in the range of  $S \sim 1$  to  $10^{-8}$  are

shown in Figure 4. Comparing with experimental data, we estimate that the sticking coefficient for NO<sub>2</sub> on PEI-coated SWNTs is  $S \sim 0.3$ , about 2 orders of magnitude higher than that on as-grown nanotubes (based on similar analysis). This clearly suggests that electron enrichment in SWNTs due to PEI functionalization significantly increases the binding affinity of NO<sub>2</sub> to the nanotubes.

The  $I-V_g$  curves for as-made n-type MT devices exhibit shapes similar to the  $\Delta G$  vs [NO<sub>2</sub>] sensing data, the two curves can be overlapped by scaling  $V_g$  or [NO<sub>2</sub>] (Figure 2b). This correlation between electrostatic and chemical gating can be used to estimate charge transfer between NO<sub>2</sub> and n-type SWNTs. The estimated gate capacitance<sup>22</sup> of our device is  $C_g \sim 1.2 \times 10^{-16}$  F for length  $L \sim 4 \mu\text{m}$  long nanotubes. Equating the amount of charges involved in chemical doping and electrostatic doping,  $\Delta Q = C_g \Delta V_g = \delta \theta (\pi d L) / \sigma$ , where  $\delta$  is the charge transfer per NO<sub>2</sub> and  $d \sim 2$  nm is tube diameter, we obtain that charge transfer is on the order of  $\delta \sim 0.1 |e|$  from an as-made PEI-coated n-type tube to adsorbed NO<sub>2</sub>, where  $e$  is the elemental charge. Note that the sticking coefficient and charge transfer estimated here are based on simplified models and are specific to the PEI-functionalized nanotubes. These parameters will depend on the doping level of SWNTs and the partial pressure of molecules in the environment.

To summarize, we have devised a strategy to fabricate large microarrays of SWNT sensor devices with 100% yield, and used polymer functionalization to enhance sensitivity and impart a certain degree of selectivity to these devices. Microspotting is used to obtain functionalized nanotube sensors in multiplex fashion that allows for selective sensing of NO<sub>2</sub> and NH<sub>3</sub>. The advances made here shall pave the way for future work in developing carbon nanotubes sensor arrays for highly sensitive and specific molecular detection and recognition in gases and in solutions.

**Acknowledgment.** This work was supported by DARPA/MTO, ABB Group Ltd., a Packard Fellowship, Sloan Fellowship, and a Dreyfus Teacher–Scholar.

## References

- (1) *Carbon Nanotubes*; Dresselhaus, M. S., Dresselhaus, G., Avouris, Ph., Eds.; Springer: Berlin, 2001; Vol. 80.
- (2) Tans, S.; Verschueren, A.; Dekker, C. *Nature* **1998**, *393*, 49–52.
- (3) Martel, R.; Schmidt, T.; Shea, H. R.; Hertel, T.; Avouris, Ph. *Appl. Phys. Lett.* **1998**, *73*, 2447–2449.
- (4) Zhou, C.; Kong, J.; Dai, H. *Appl. Phys. Lett.* **1999**, *76*, 1597.
- (5) Dai, H. *Acc. Chem. Res.* **2002**, *35*, 1035–1044.
- (6) Kong, J.; Franklin, N.; Zhou, C.; Chapline, M.; Peng, S.; Cho, K.; Dai, H. *Science* **2000**, *287*, 622–625.
- (7) Kong, J.; Dai, H. *J. Phys. Chem.* **2001**, *105*, 2890–2893.
- (8) Kong, J.; Soh, H.; Cassell, A.; Quate, C. F.; Dai, H. *Nature* **1998**, *395*, 878.
- (9) Franklin, N. R.; Wang, Q.; Tomblor, T. W.; Javey, A.; Shim, M.; Dai, H. *Appl. Phys. Lett.* **2002**, *81*, 913–915.
- (10) Kim, W.; Choi, H. C.; Shim, M.; Li, Y.; Wang, D.; Dai, H. *Nano Lett.* **2002**, *2*, 703–708.
- (11) Collins, P. G.; Fuhrer, M. S.; Zettl, A. *Appl. Phys. Lett.* **2000**, *76*, 894–896.
- (12) Shim, M.; Javey, A.; Kam, N. W. S.; Dai, H. *J. Am. Chem. Soc.* **2001**, *123*, 11512–11513.
- (13) Chen, R.; Franklin, N.; Kong, J.; Cao, J.; Tomblor, T.; Zhang, Y.; Dai, H. *Appl. Phys. Lett.* **2001**, *79*, 6951.
- (14) Thornton, J. A.; Wooldridge, P. J.; Cohen, R. C. *Anal. Chem.* **2000**, *72*, 528–539.
- (15) He, Y. K.; Cussler, E. L. *J. Membr. Sci.* **68**, 43–52.
- (16) Peng, S.; Cho, K. *Nanotechnology* **2000**, *11*, 57.
- (17) Chang, H.; Lee, J.; Lee, S.; Lee, Y. *Appl. Phys. Lett.* **2001**, *79*, 3863–3865.
- (18) Long, R. T.; Yang, R. T. *Ind. Eng. Chem. Res.* **2001**, *40*, 4288–4291.
- (19) Zhao, J. J.; Buldum, A.; Han, J.; Lu, J. P. *Nanotechnology* **2002**, *13*, 195–200.
- (20) Goldoni, A.; Larciprete, R.; Petaccia, L.; Lizzit, S., unpublished results.
- (21) Somorjai, G. A. *Introduction to Surface Chemistry and Catalysis*; John Wiley and Sons: New York, 1994.
- (22) Javey, A.; Kim, H.; Brink, M.; Wang, Q.; Ural, A.; McIntyre, P.; McEuen, P.; Dai, H. *Nature Mater.* **2002**, *1*, 241–246.

NL034010K